Supporting Information

Selective Synthesis of Iridium(III) End-Capped Polyynes by Oxidative Addition of 1-Iodopolyynes to Vaska's Complex

*Bartłomiej Pigulski. Agata Jarszak, Sławomir Szafert**

Faculty of Chemistry, University of Wrocław, 14 F. Joliot-Curie, 50-383 Wrocław, Poland

Table of contents

X-ray Crystallography Details 3

UV/Vis Spectra 5

DFT Calculations Details 7

Cyclic Voltammetry 10

NMR Spectra 10

X-ray Crystallography Details

Table S1. Details of X-ray single crystal diffraction experiment for **2**-C_4[Ir]I·C_7H_8

2-C_4[Ir]I	
Chemical formula	$C_{47}H_{34}ClIIrNO_3P_2 \cdot C_7H_8$
M_r	1169.37
Crystal system, space group	Monoclinic, $P2_1/n$
Temperature (K)	100
a, b, c (Å)	10.424 (3), 14.820 (5), 30.152 (9)
β (°)	94.81 (3)
V (Å^3)	4642 (2)
Z	4
Radiation type	Mo $K\alpha$
μ (mm^{-1})	3.71
Crystal size (mm)	0.17 × 0.06 × 0.04
Data collection	
Diffractometer	KUMA KM-4 CCD
Absorption correction	Analytical *CrysAlis PRO*, Oxford Diffraction Ltd., Version 1.171.33.66 (release 28-04-2010 CrysAlis171 .NET) (compiled Apr 28 2010,14:27:37) Analytical numeric absorption correction using a multifaceted crystal model based on expressions derived by R.C. Clark & J.S. Reid. (Clark, R. C. & Reid, J. S. (1995). Acta Cryst. A51, 887-897)
T_{min}, T_{max}	0.679, 0.885
No. of measured, independent and observed reflections	37593, 12946, 5253 $\{I > 2\sigma(I)\}$
R_{int}	0.163
$(\sin \theta/\lambda)_{max}$ (Å^{-1})	0.845
Refinement	
$R[F^2 > 2\sigma(F^2)]$, $wR(F^2)$, S	0.061, 0.124, 0.76
No. of reflections	12946
No. of parameters	540
No. of restraints	76
H-atom treatment	H-atom parameters constrained
$\Delta\rho_{max}$, $\Delta\rho_{min}$ (e Å^{-3})	1.62, −1.83

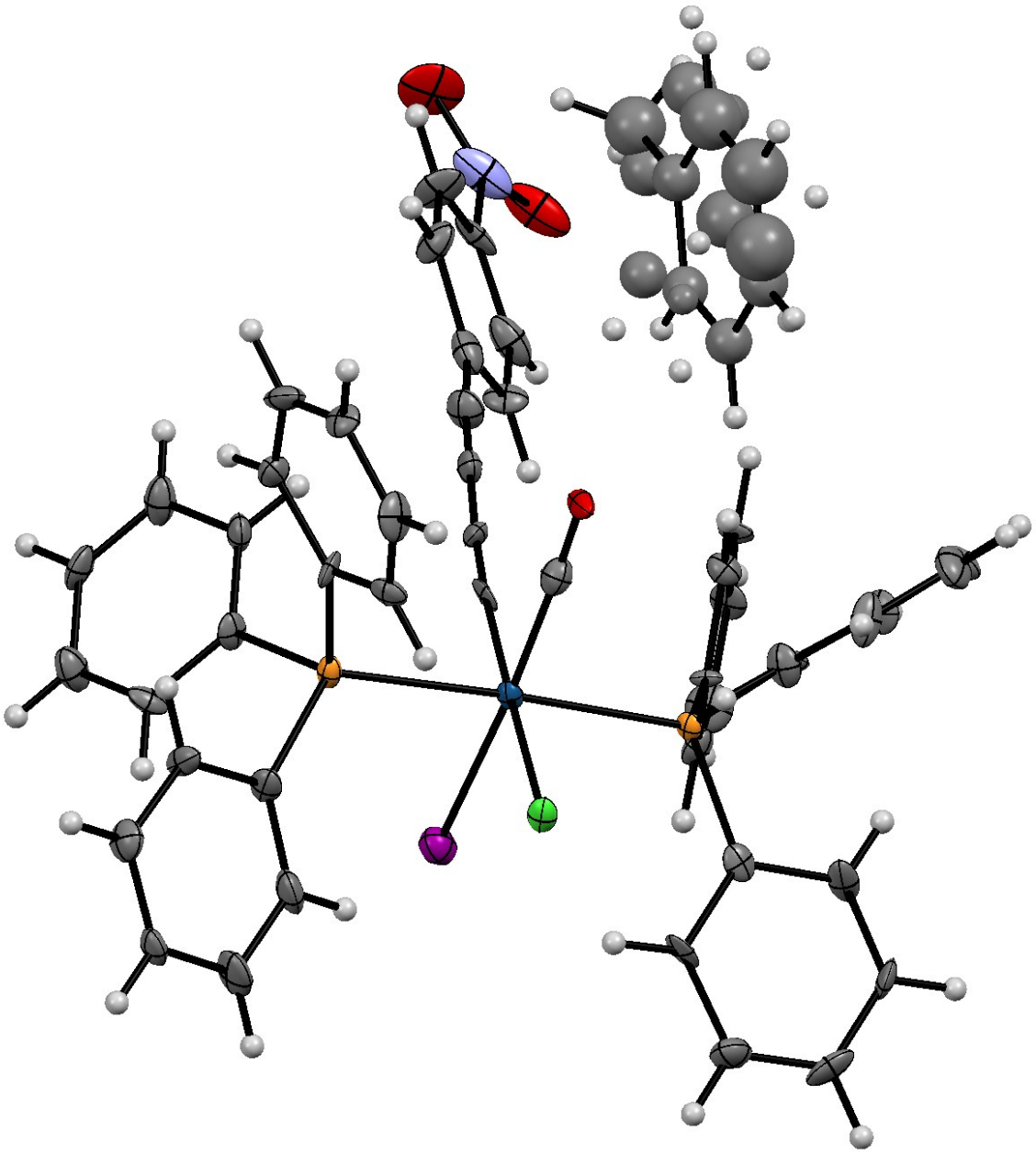

Figure S1. Molecular structure of **2**-C_4[Ir]I·C_7H_8. Thermal ellipsoids are given with 50% probability.

UV/Vis Spectra

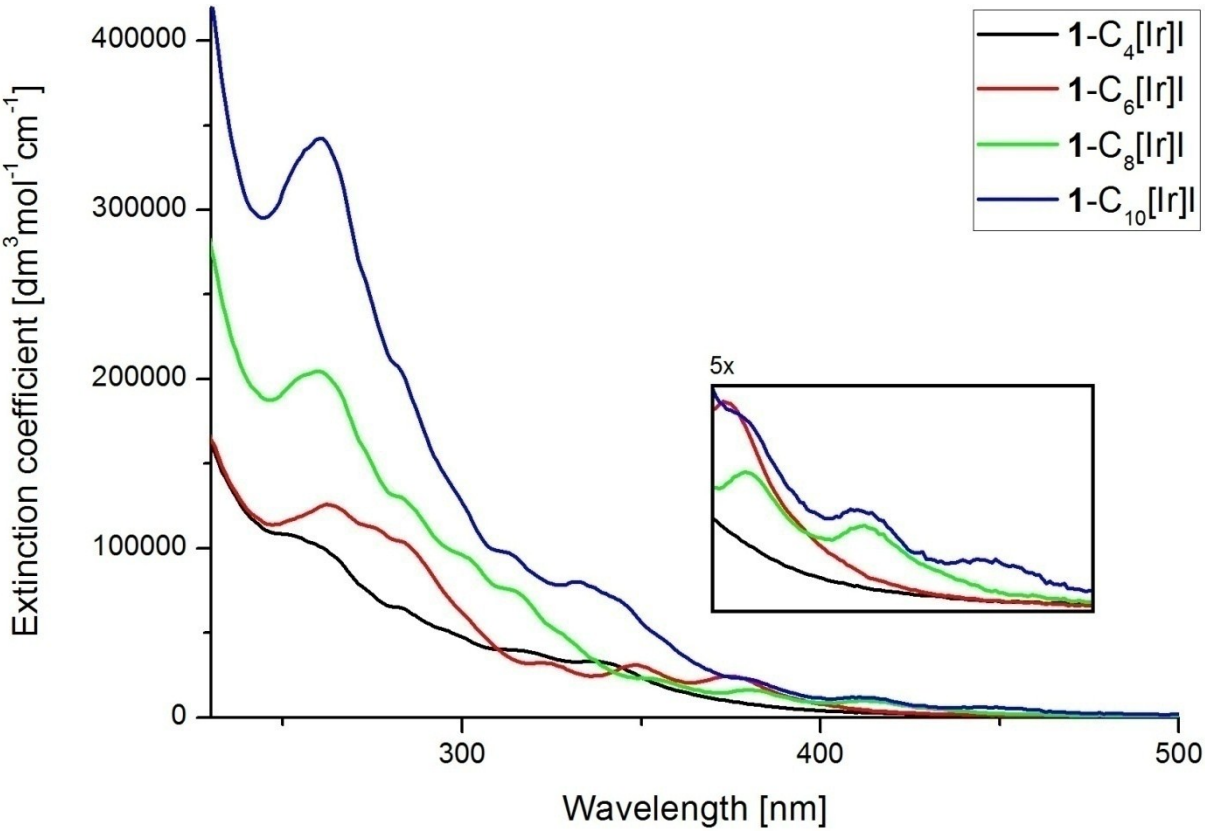

Figure S2. UV-Vis spectra of **1**-$C_{4\text{-}10}$[Ir]I polyynes.

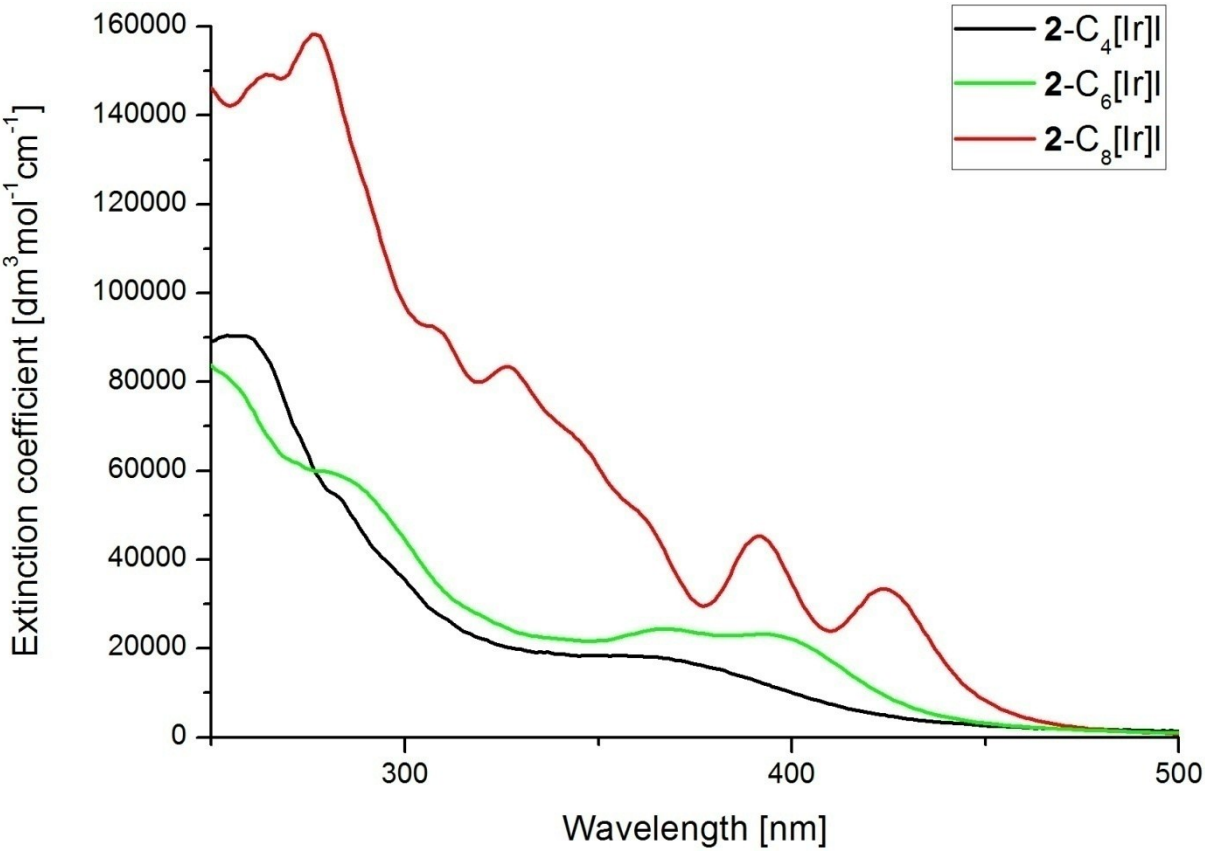

Figure S3. UV-Vis spectra of **2**-$C_{4\text{-}8}$[Ir]I polyynes.

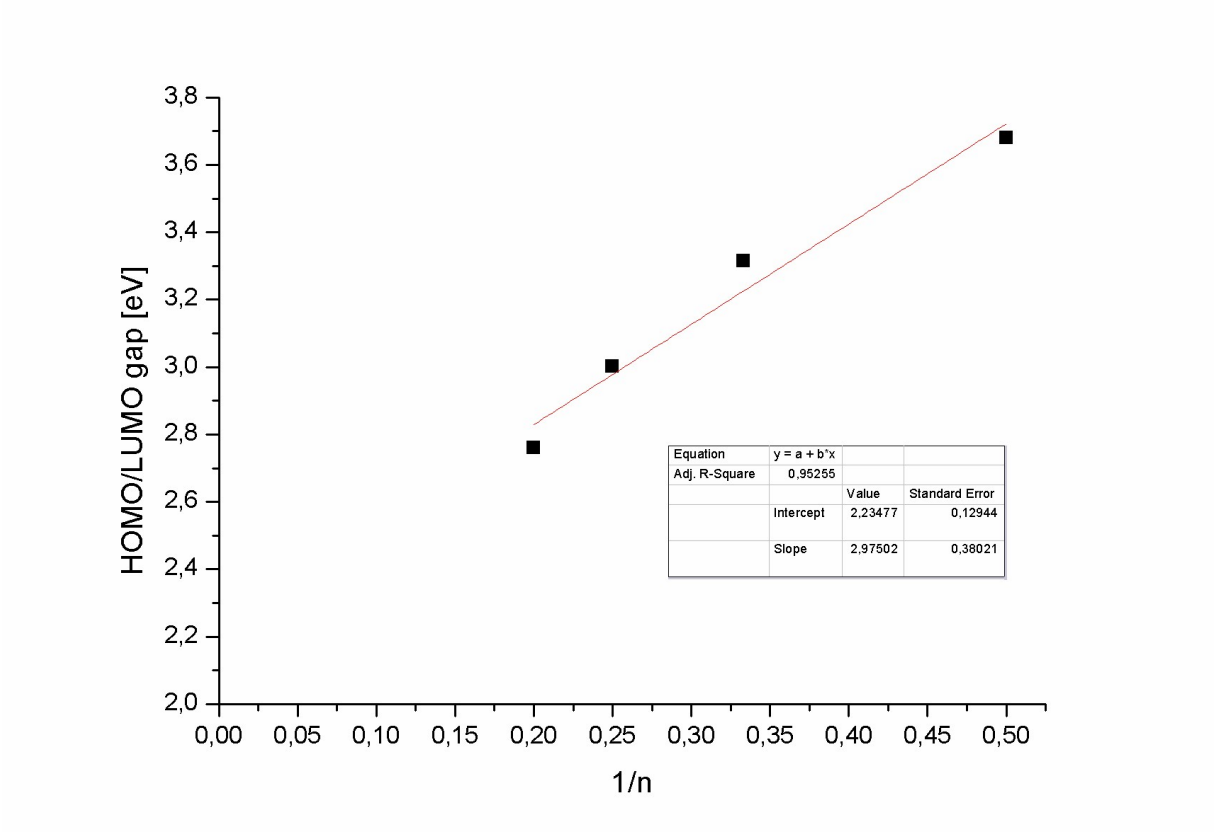

Figure S4. Plot of HOMO/LUMO gap calculated from UV/Vis spectra versus n (n = number of triple bonds) for **1**-C_n[Ir]I series of complexes**.**

DFT Calculations Details

Table S2. HOMO and HOMO-1 orbitals.

	HOMO-1	HOMO
1-C_4[Ir]I	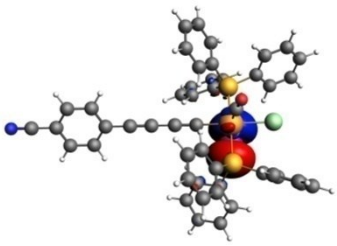	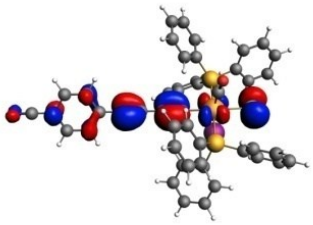
1-C_6[Ir]I	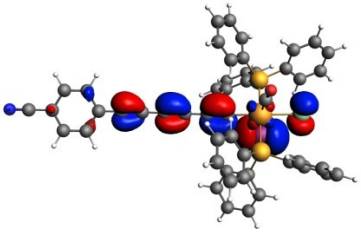	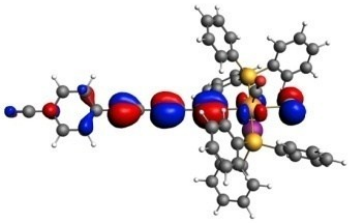
1-C_8[Ir]I	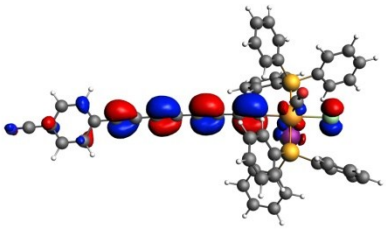	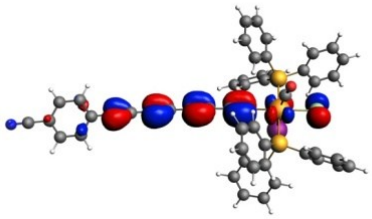
1-C_{10}[Ir]I	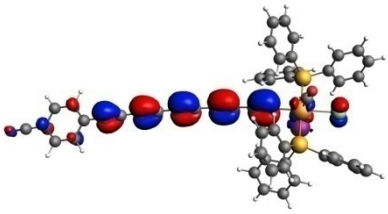	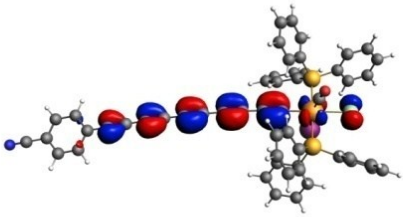
2-C_4[Ir]I	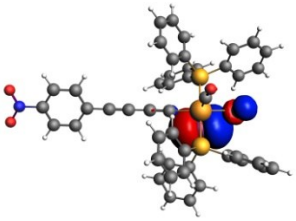	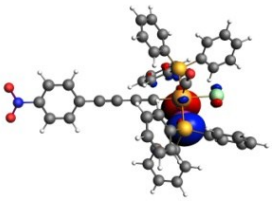
2-C_6[Ir]I	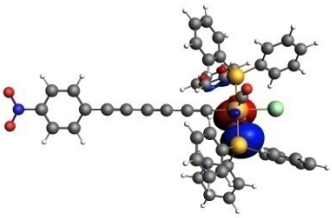	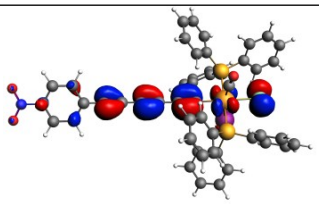
2-C_8[Ir]I	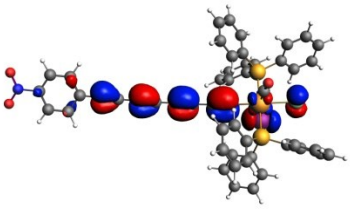	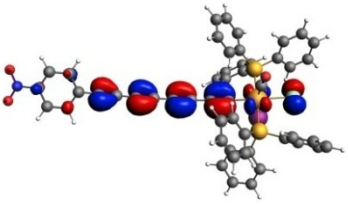

Table S3. LUMO and LUMO+1 orbitals.

	LUMO	LUMO+1
1-C_4[Ir]I	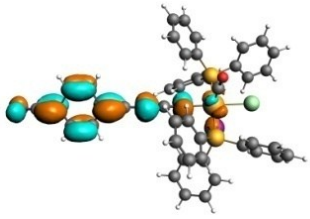	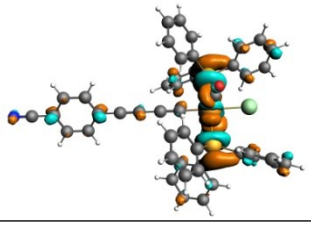
1-C_6[Ir]I	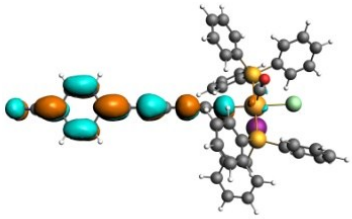	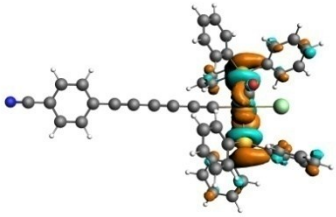
1-C_8[Ir]I	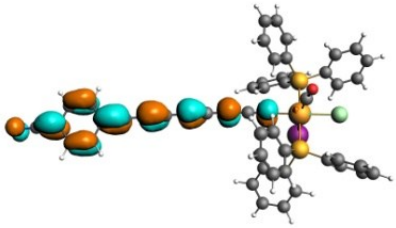	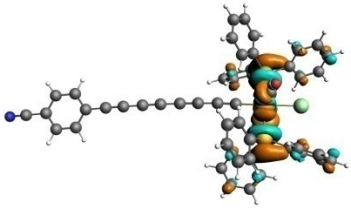
1-C_{10}[Ir]I	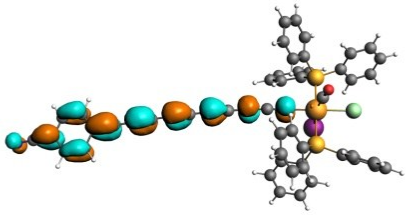	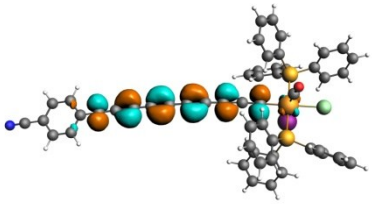
2-C_4[Ir]I	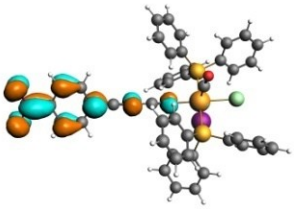	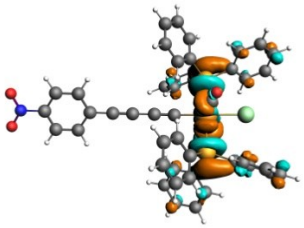
2-C_6[Ir]I	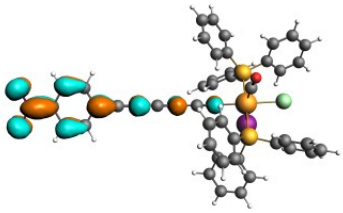	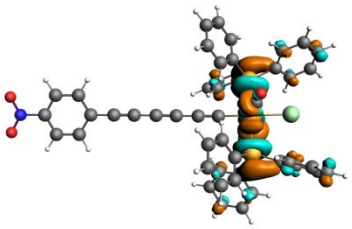
2-C_8[Ir]I	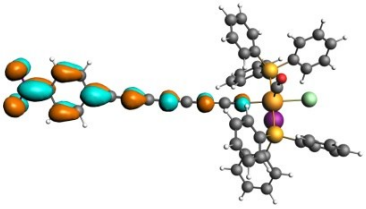	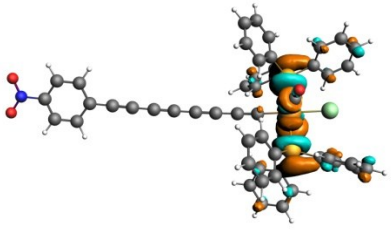

Table S4. Energies of frontier molecular orbitals.

	HOMO-1 [eV]	HOMO [eV]	LUMO [eV]	LUMO+1 [eV]	HOMO/LUMO gap [eV]
1-C_4[Ir]I	-5.33	-5.28	-2.87	-2.82	2.41
1-C_6[Ir]I	-5.32	-5.26	-3.10	-2.85	2.16
1-C_8[Ir]I	-5.27	-5.24	-3.28	-2.92	1.96
1-C_{10}[Ir]I	-5.23	-5.22	-3.44	-3.05	1.78
2-C_4[Ir]I	-5.33	-5.32	-3.51	-2.85	1.81
2-C_6[Ir]I	-5.35	-5.31	-3.61	-2.90	1.70
2-C_8[Ir]I	-5.36	-5.29	-3.70	-2.94	1.59

Cyclic Voltammetry

Table S5. Potentials of reduction and oxidation peaks versus SCE ($E_{1/2}$ ferrocenium/ferrocene (Fc+ /Fc) redox couple = 0.520 V vs. SCE in $CH_2Cl_2/(Bu_4N)[PF_6]$)).

Compound	E_p^{red}	E_p^{ox}
1-C_{10}[Ir]I	-1.576	1.198
2-C_4[Ir]I	-1.646	-1.055
2-C_6[Ir]I	-1.224, -1.519	-1.235, -0.984
2-C_8[Ir]I	-1.133; -1.421	-1.211, -0.943

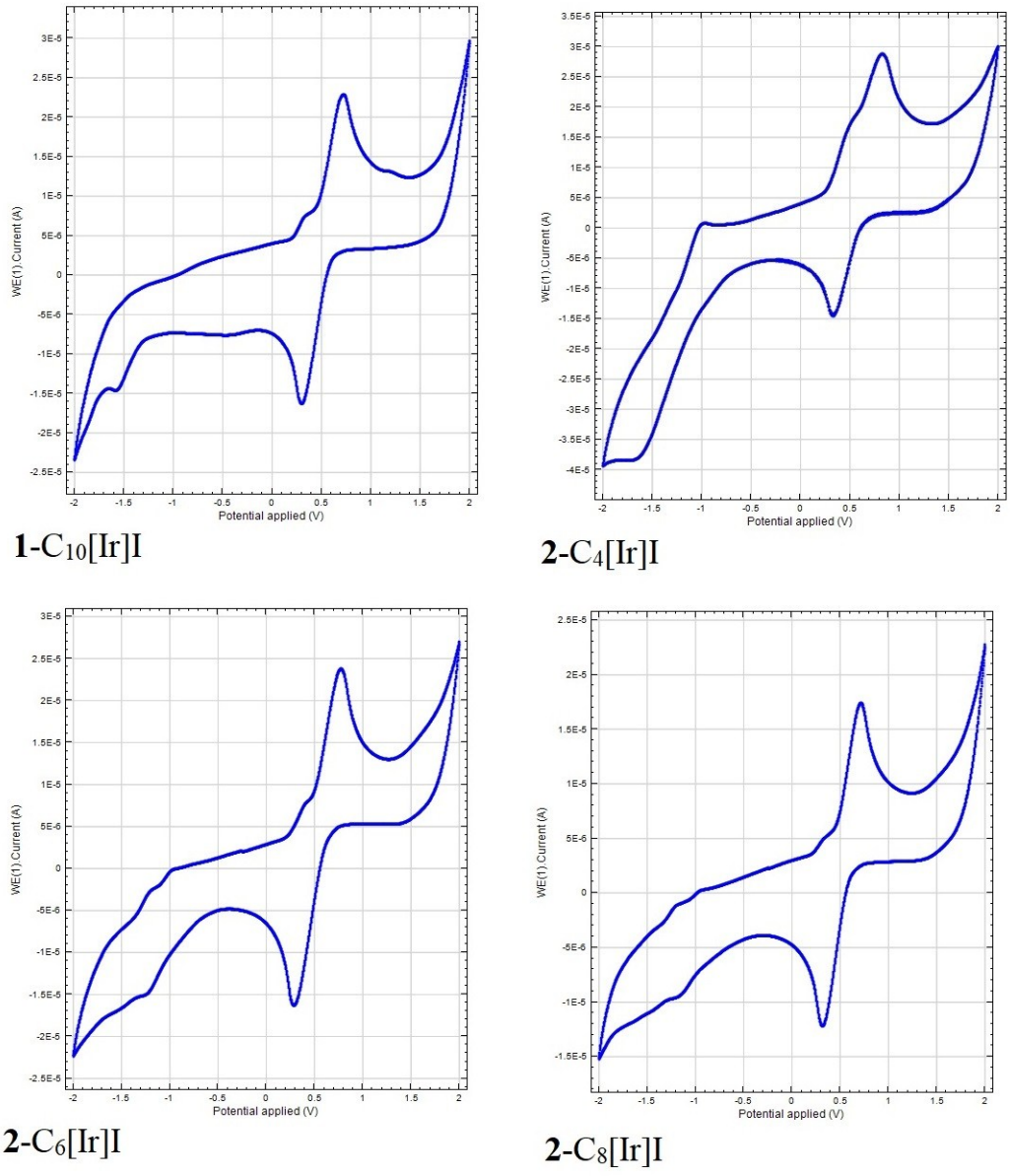

Figure S4. Cyclic voltammograms of **1**-C_{10}[Ir]I, **2**-C_4[Ir]I, **2**-C_6[Ir]I, **2**-C_8[Ir]I with added ferrocene.

NMR Spectra

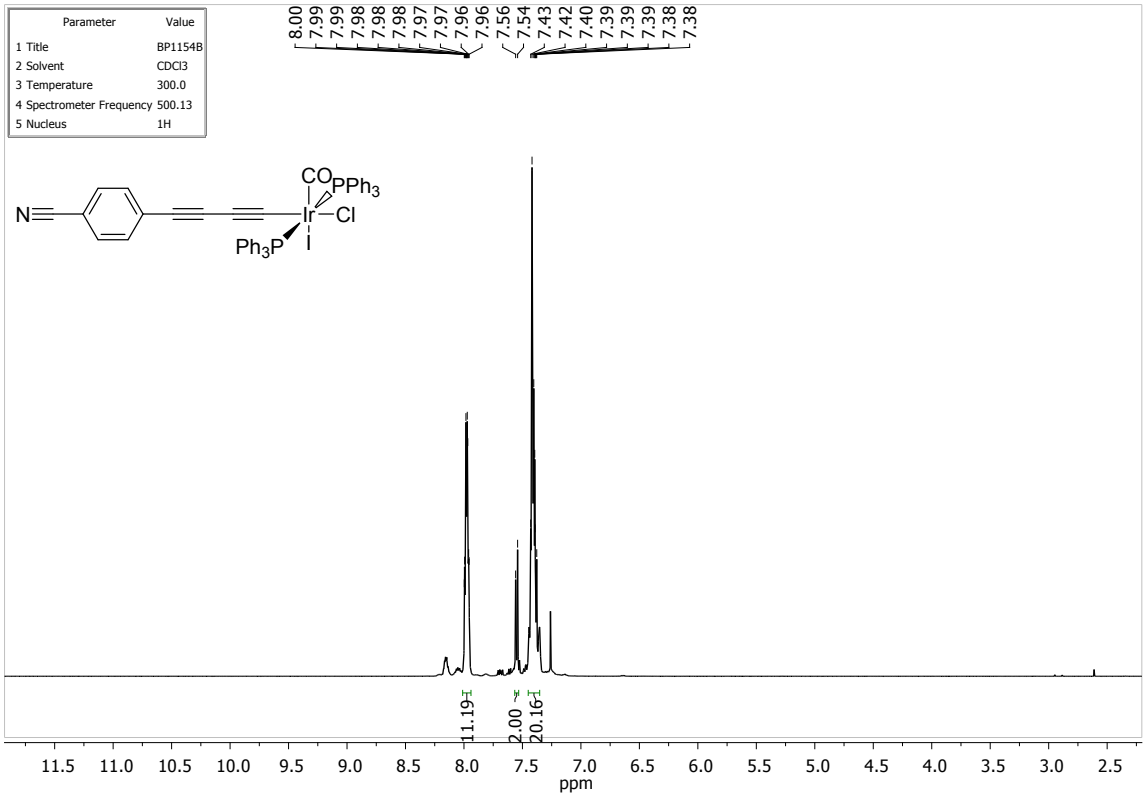

Figure S5. ^{1}H NMR spectrum of **1**-C_4[Ir]I.

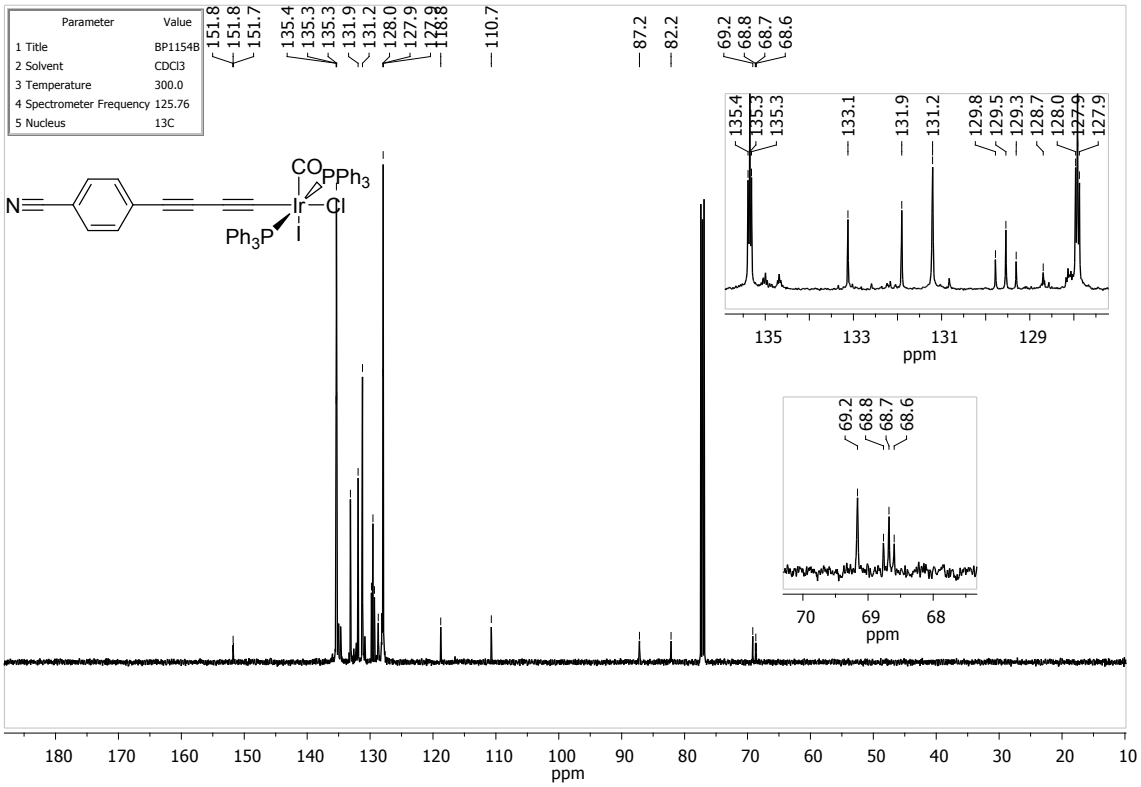

Figure S6. ^{13}C NMR spectrum of **1**-C_4[Ir]I.

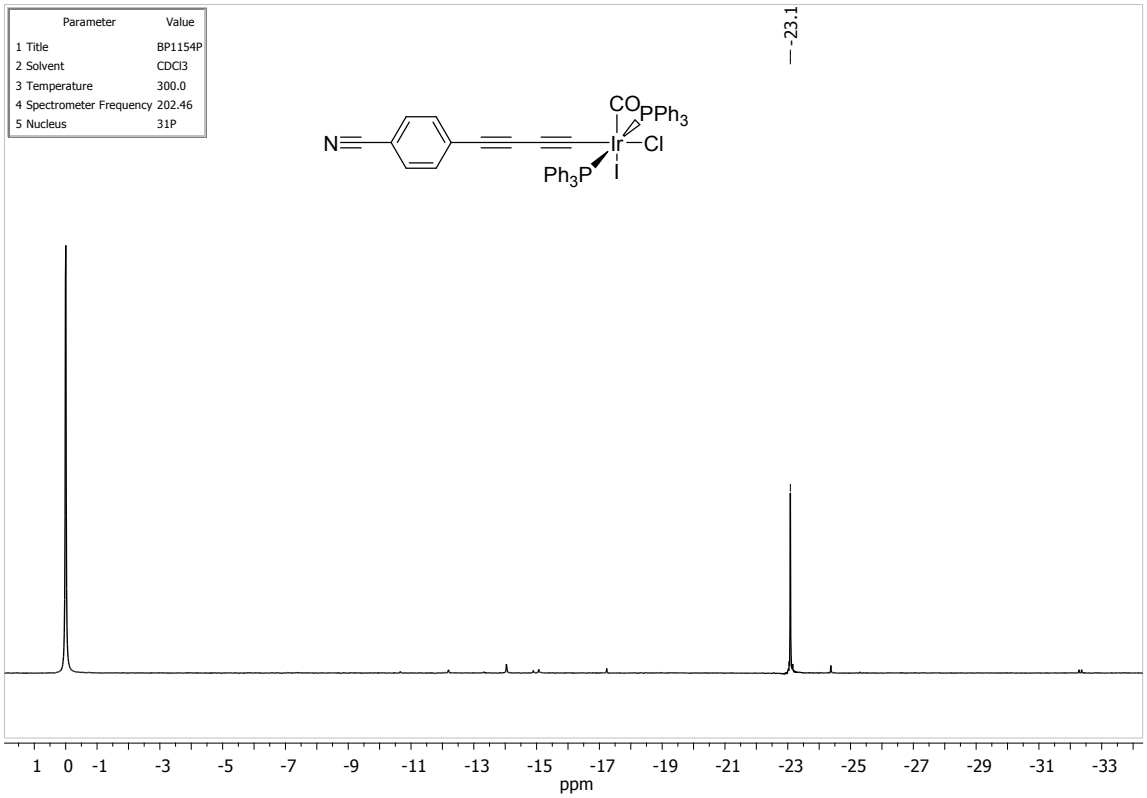

Figure S7. ^{31}P NMR spectrum of **1**-C_4[Ir]I.

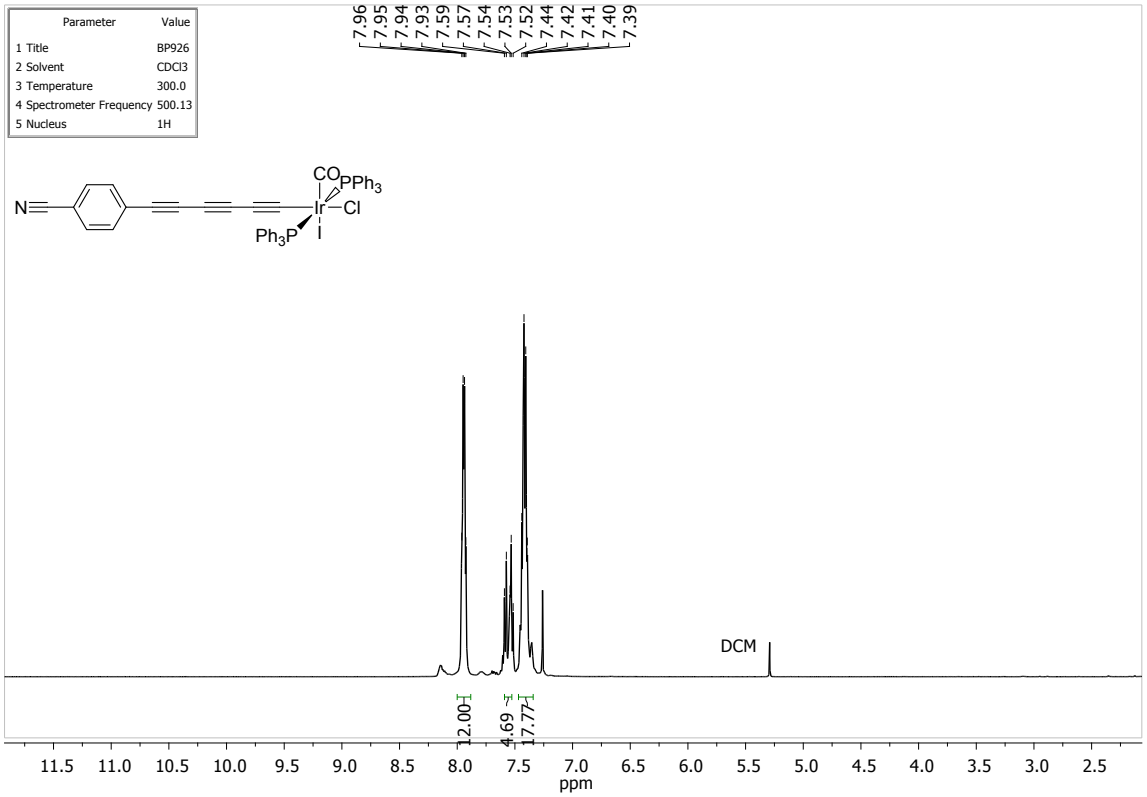

Figure S8. ^{1}H NMR spectrum of **1**-C_6[Ir]I.

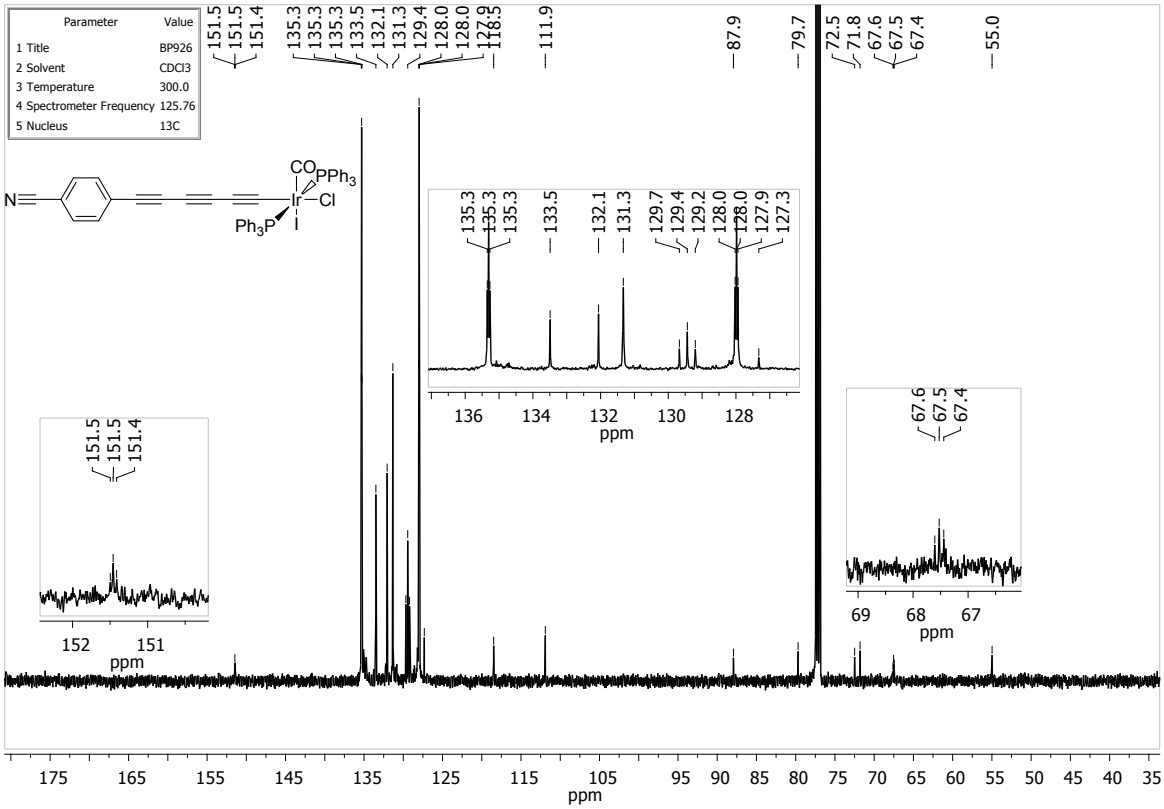

Figure S9. ^{13}C NMR spectrum of **1**-C_6[Ir]I.

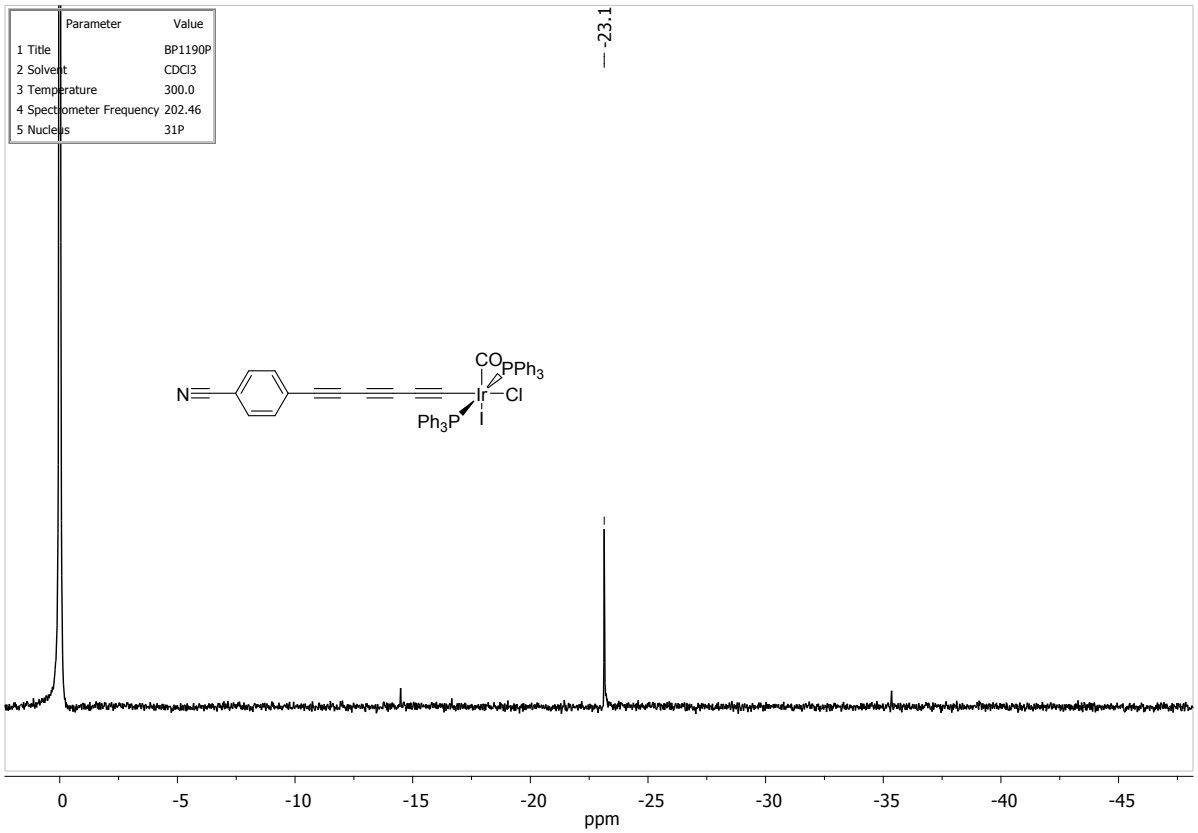

Figure S10. ^{31}P NMR spectrum of **1**-C_6[Ir]I.

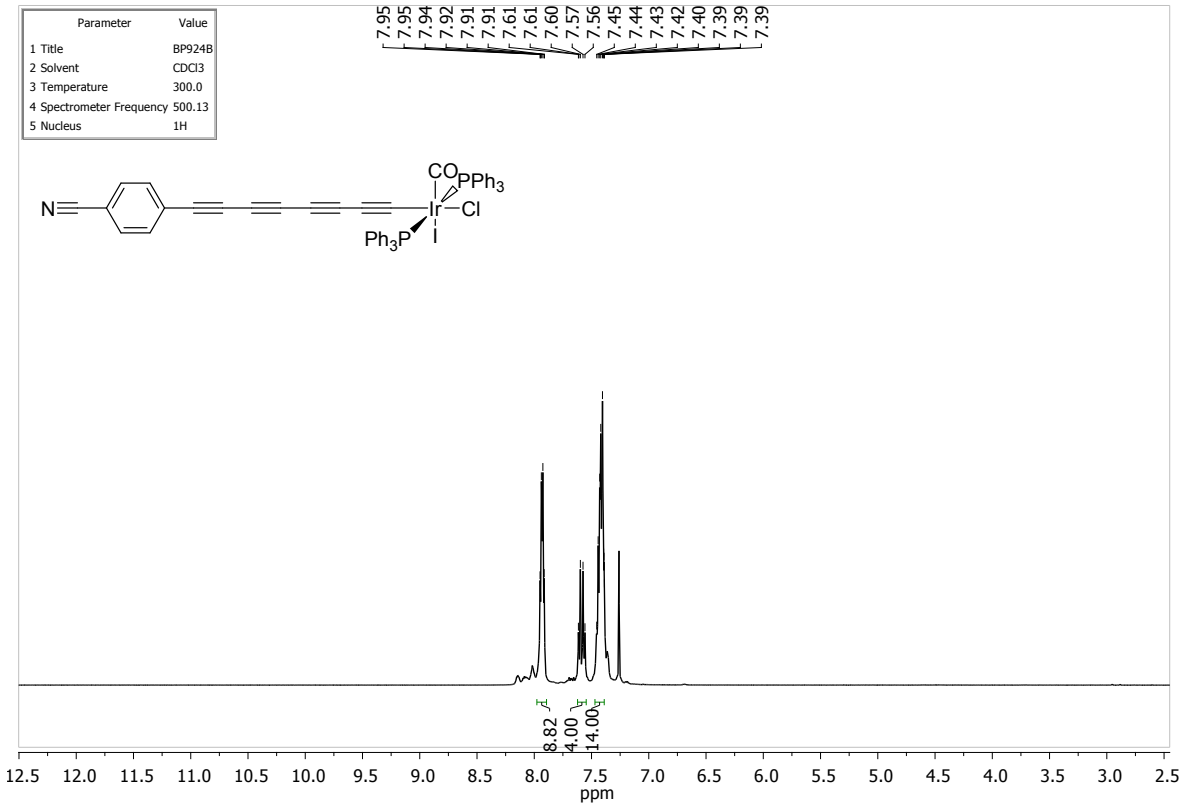

Figure S11. ^{1}H NMR spectrum of **1**-C_8[Ir]I.

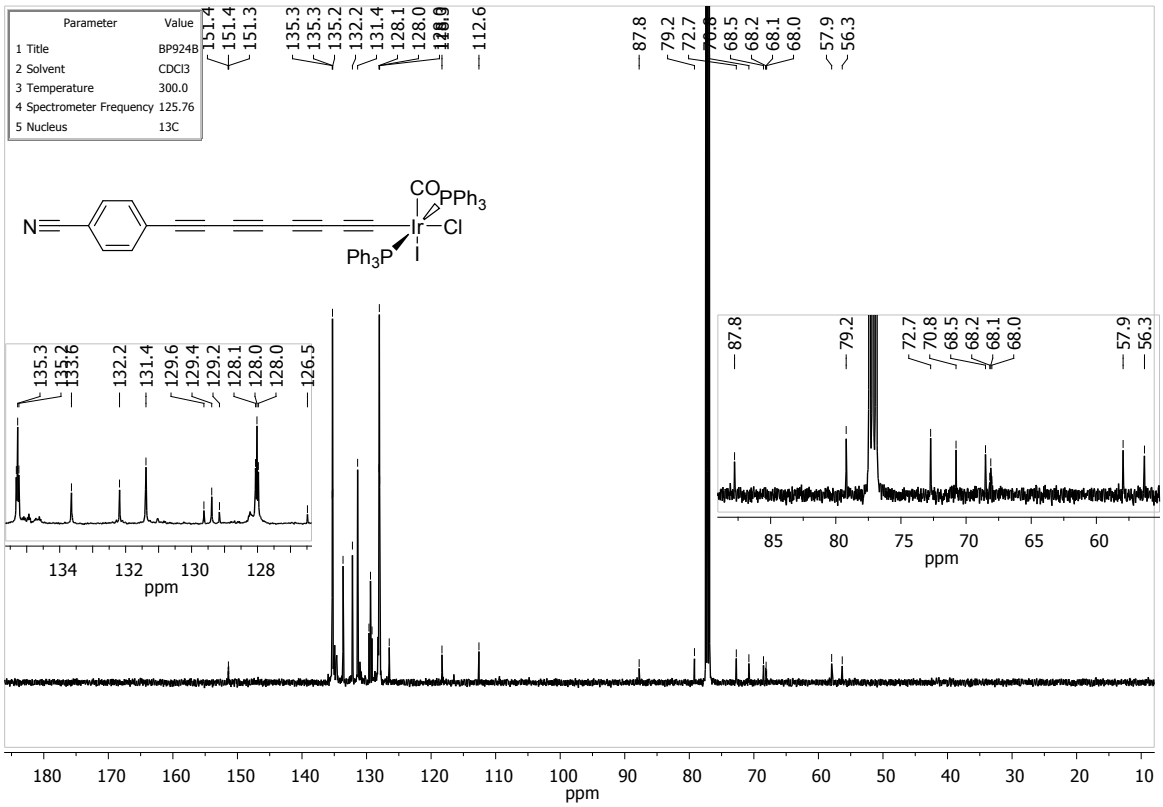

Figure S12. ^{13}C NMR spectrum of **1**-C_8[Ir]I.

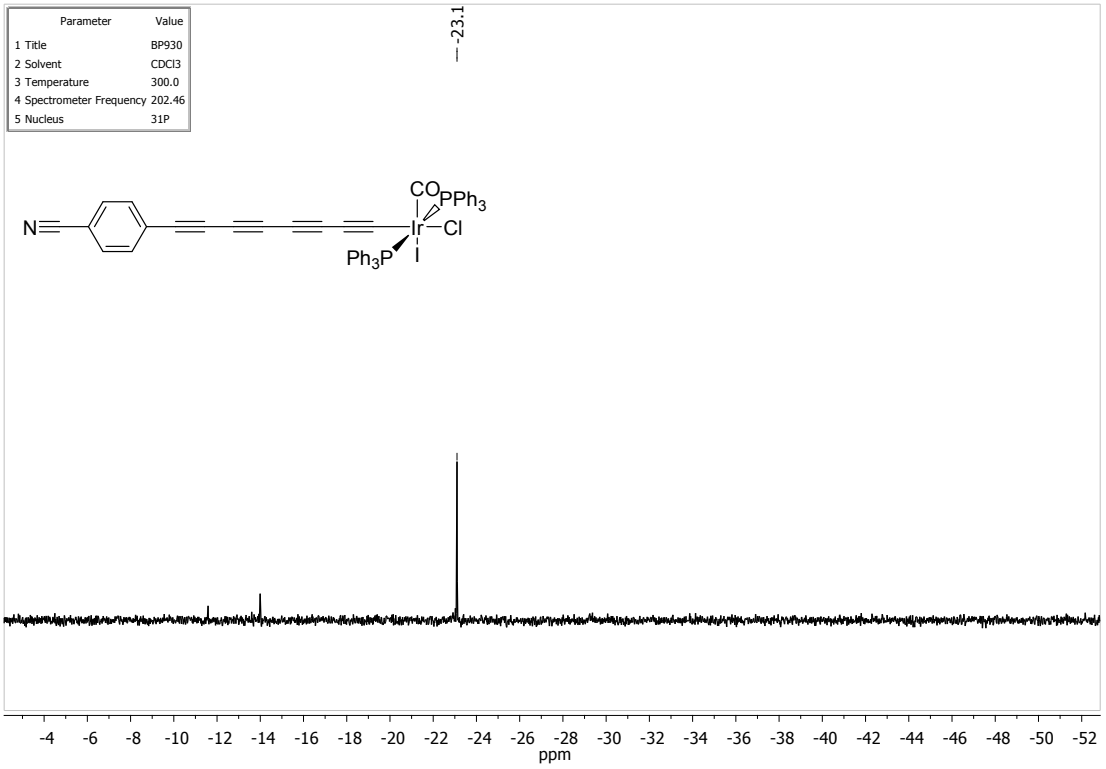

Figure S13. ^{31}P NMR spectrum of **1**-C_8[Ir]I.

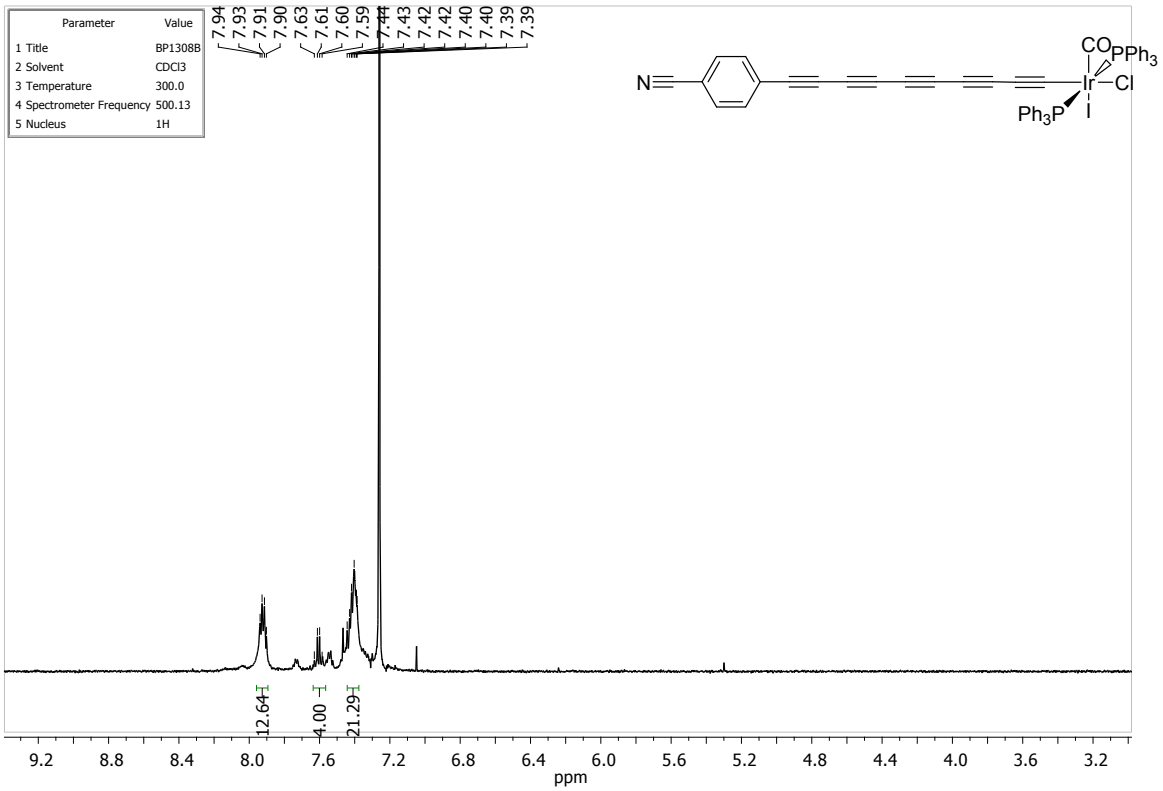

Figure S14. ^{1}H NMR spectrum of **1**-C_{10}[Ir]I.

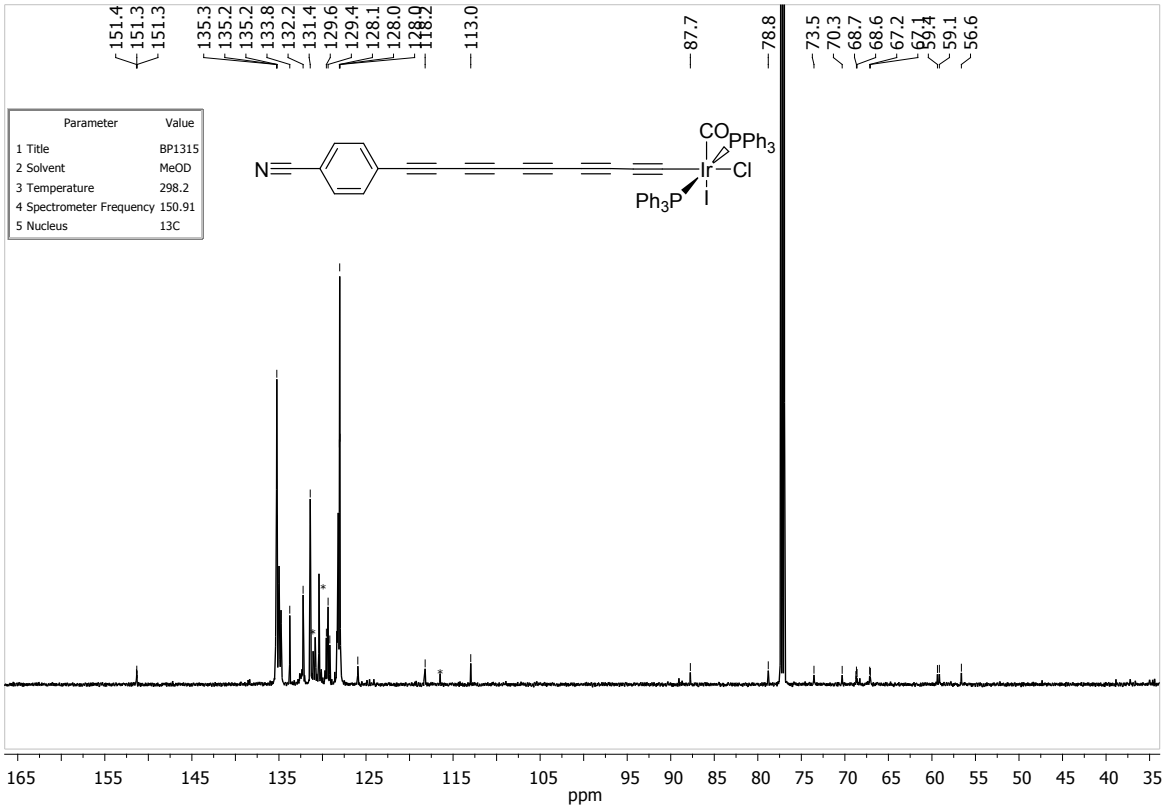

Figure S15. ^{13}C NMR spectrum of **1**-C_{10}[Ir]I.

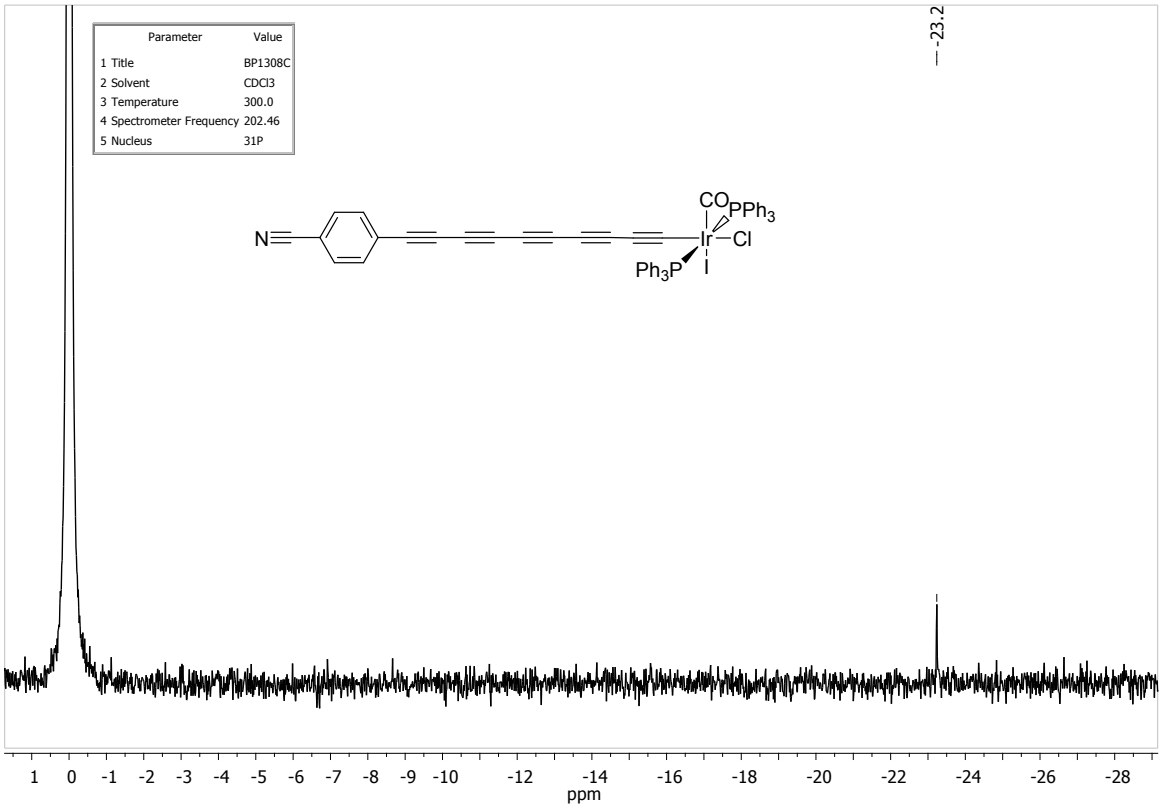

Figure S16. ^{31}P NMR spectrum of **1**-C_{10}[Ir]I.

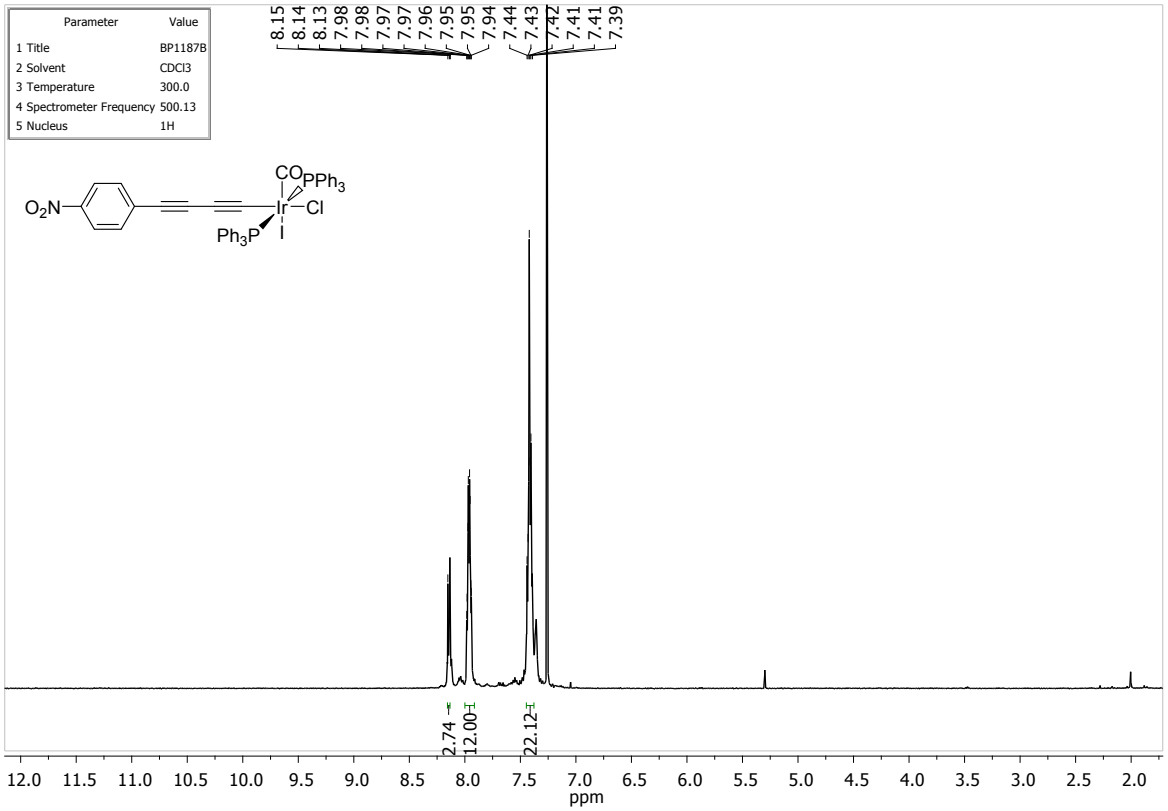

Figure S17. ^{1}H NMR spectrum of **2**-C_4[Ir]I.

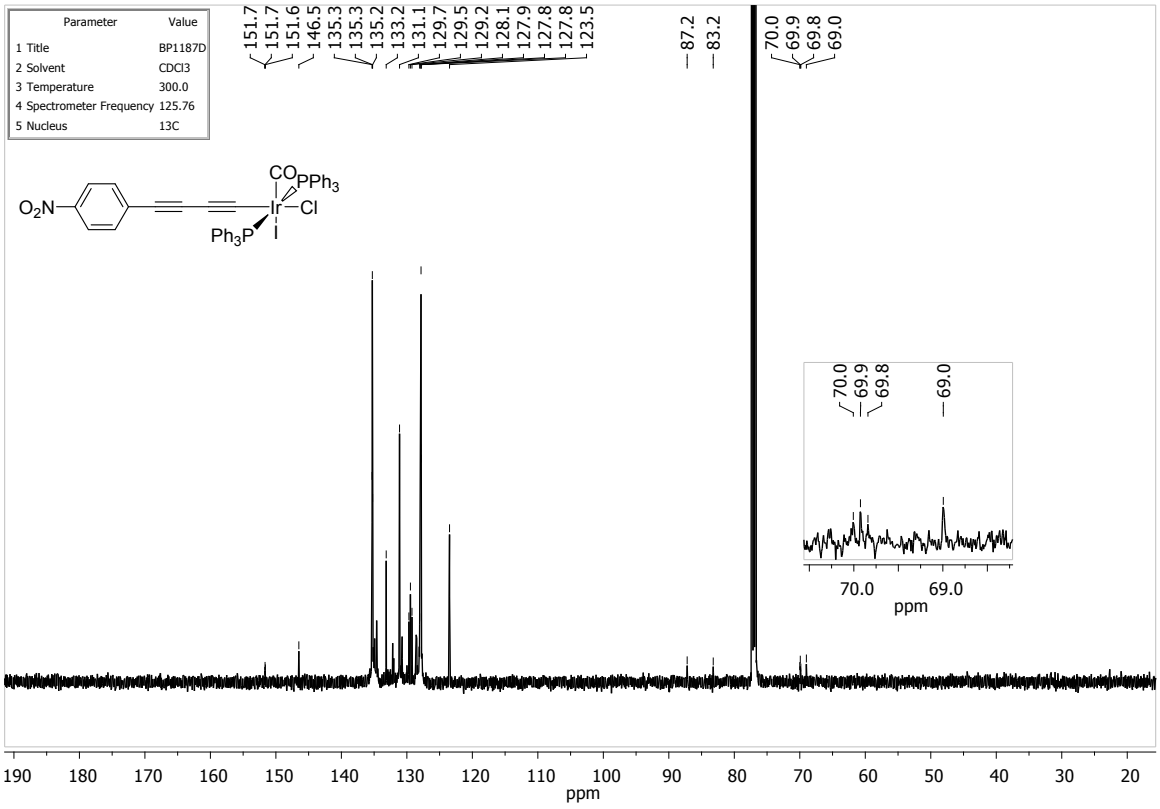

Figure S18. ^{13}C NMR spectrum of **2**-C_4[Ir]I.

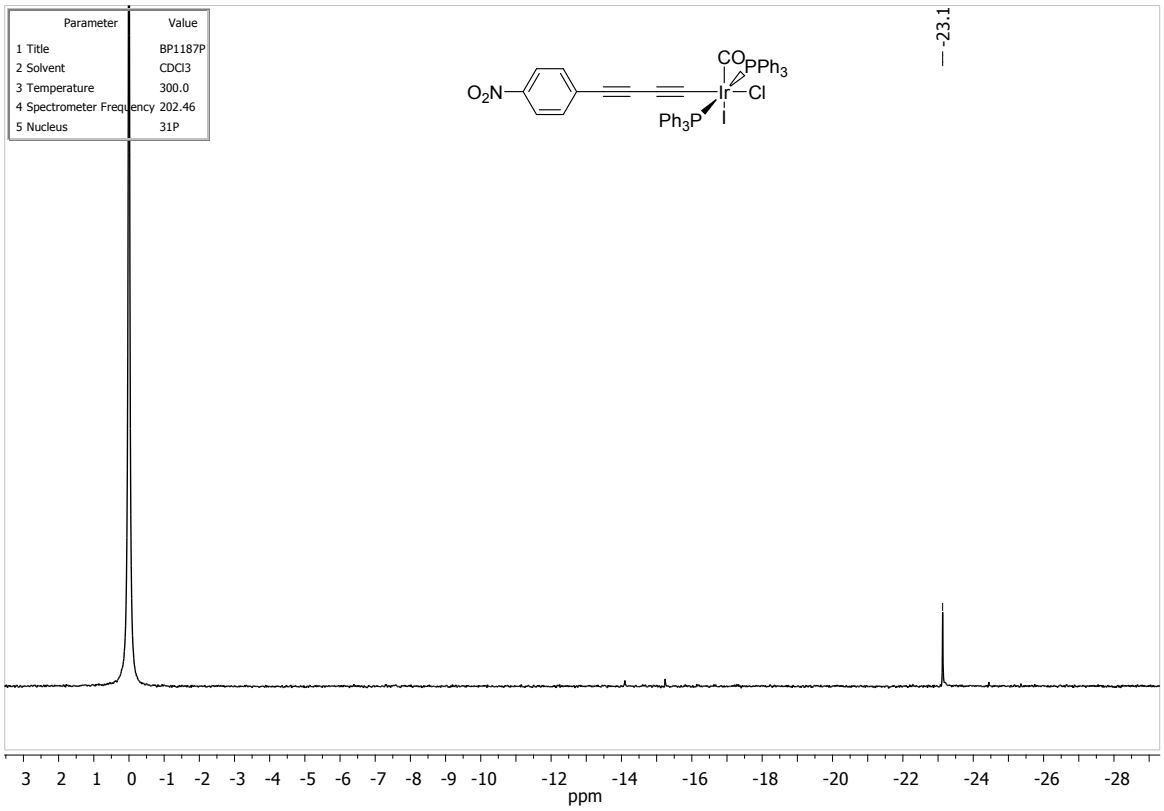

Figure S19. ^{31}P NMR spectrum of **2**-C_4[Ir]I.

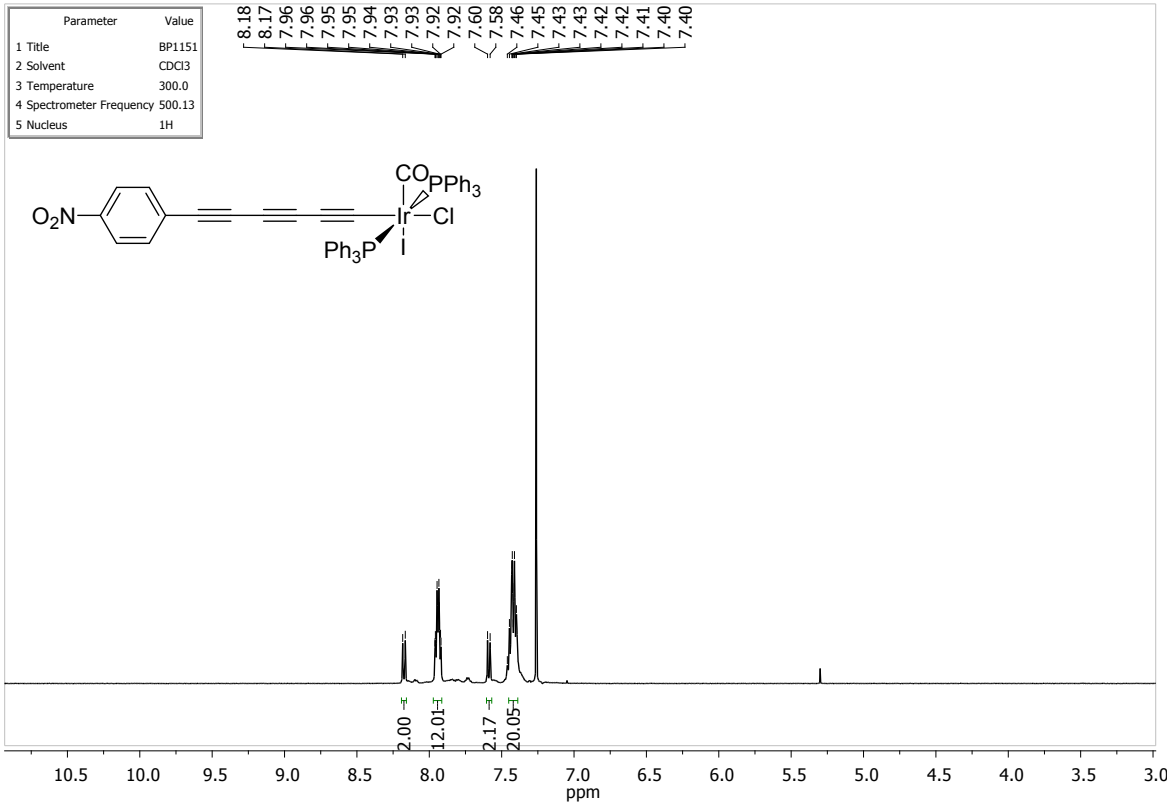

Figure S20. ^{1}H NMR spectrum of **2**-C_6[Ir]I.

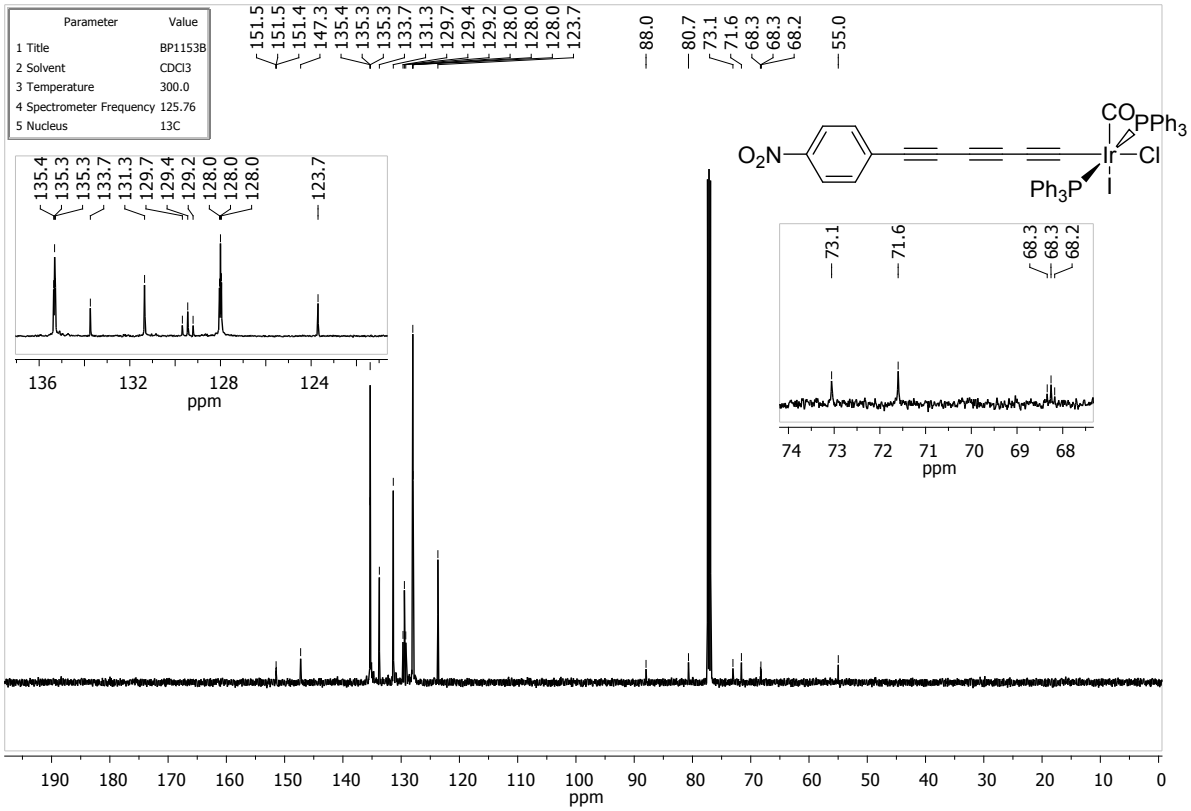

Figure S21. ^{13}C NMR spectrum of **2**-C_6[Ir]I.

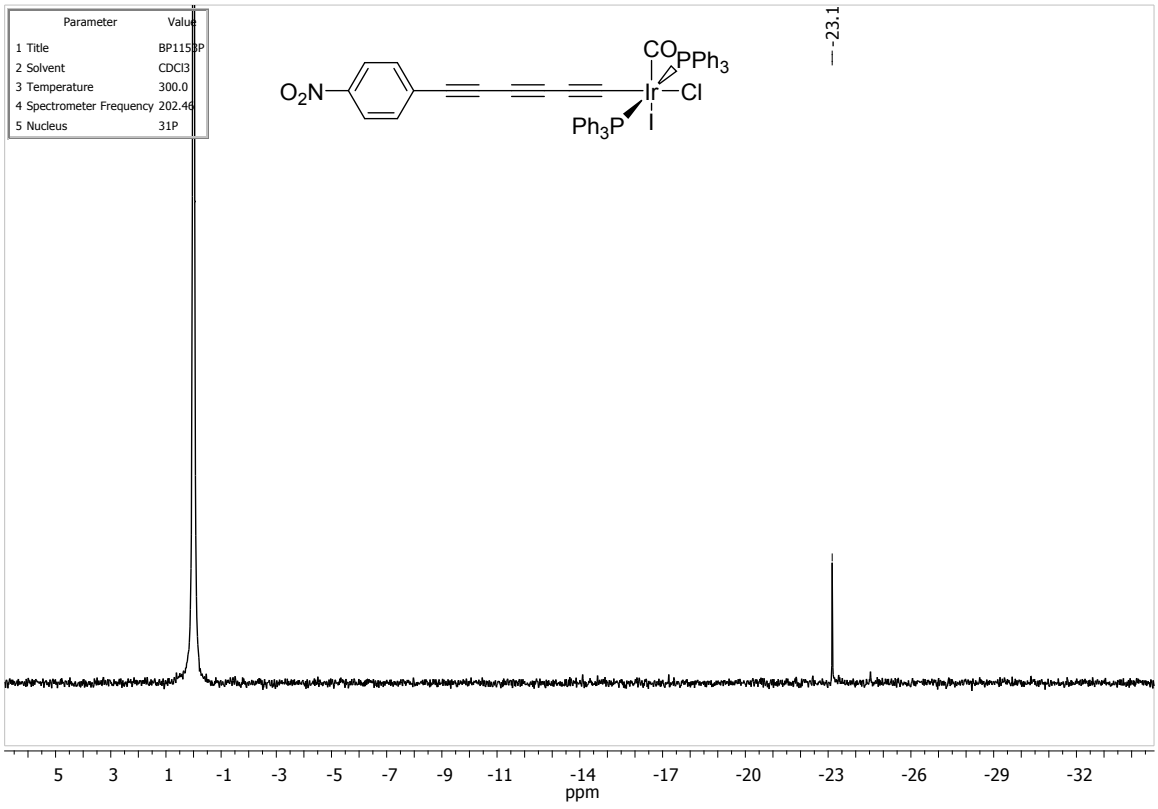

Figure S22. ^{31}P NMR spectrum of **2**-C_6[Ir]I.

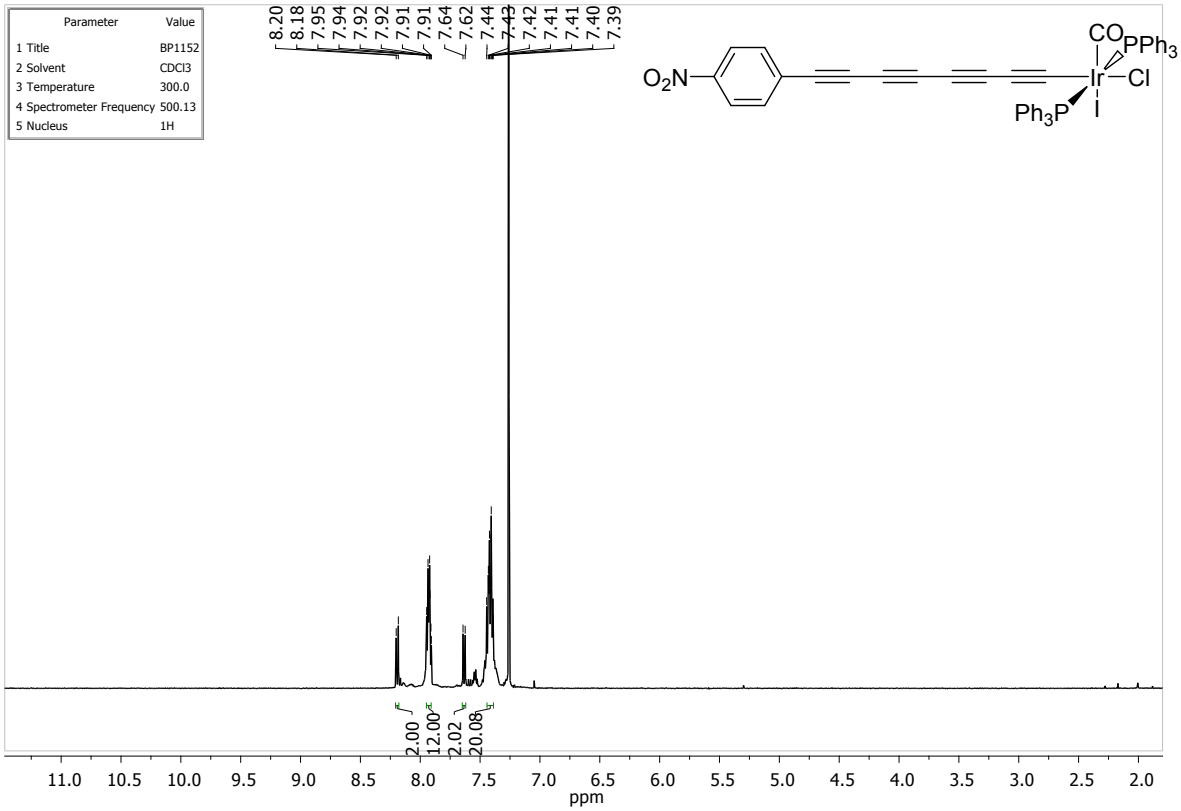

Figure S23. ^{1}H NMR spectrum of **2**-C_8[Ir]I.

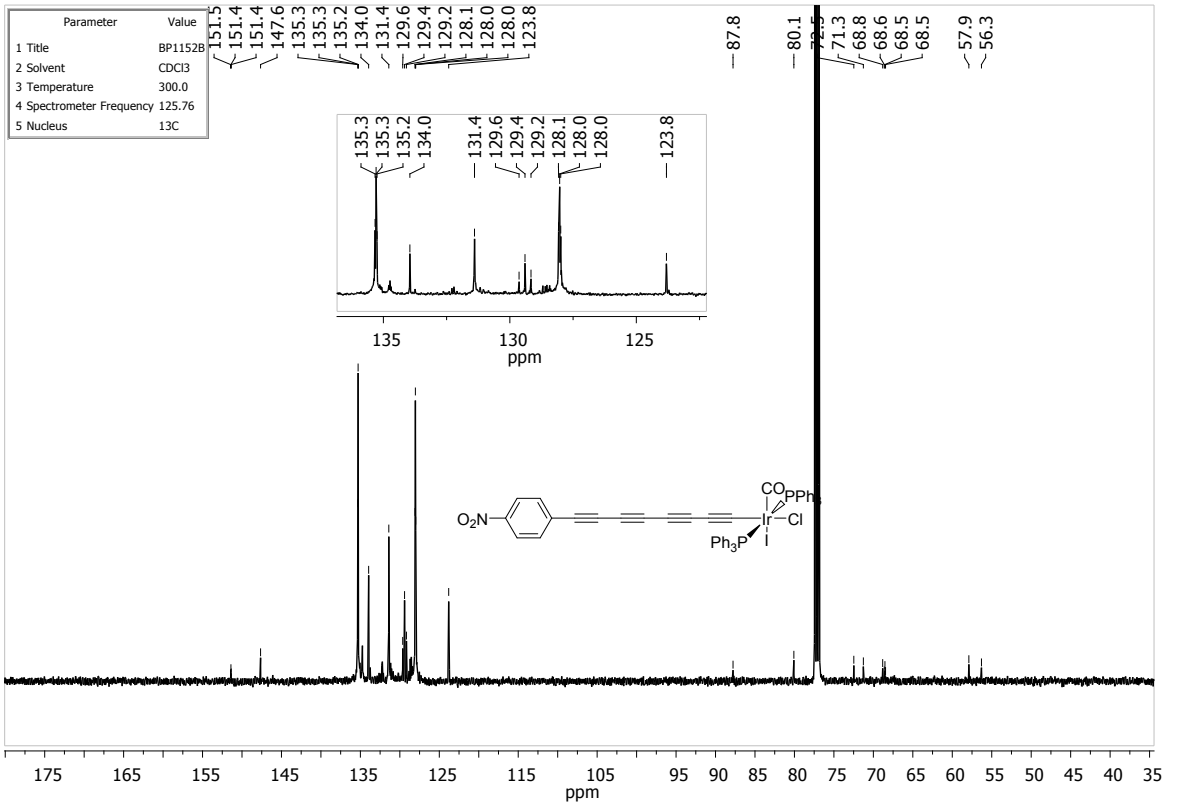

Figure S24. ^{13}C NMR spectrum of **2**-C_8[Ir]I.

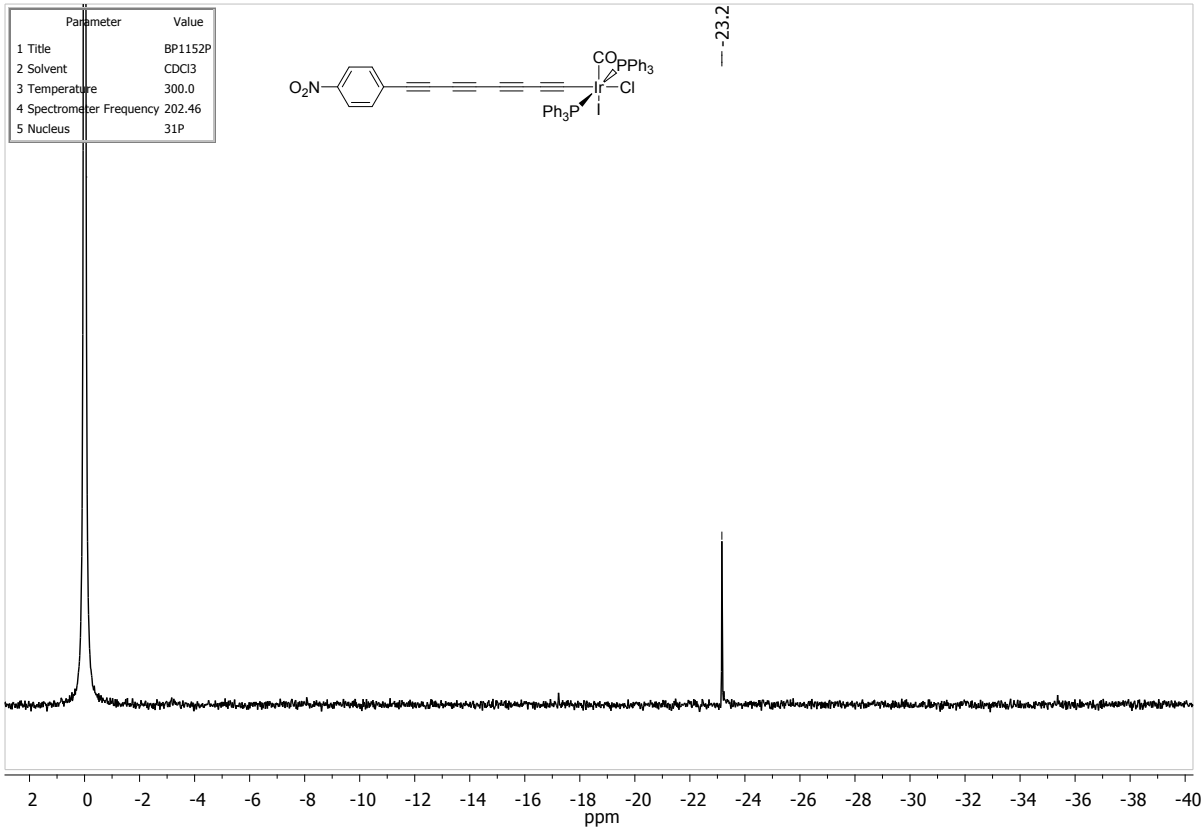

Figure S25. ^{31}P NMR spectrum of **2**-C_8[Ir]I.